International Journal of Thermal Sciences 49 (2010) 161–169

Contents lists available at ScienceDirect

International Journal of Thermal Sciences

journal homepage: www.elsevier.com/locate/ijts

3D study of cooling system effect on the heat transfer during polymer injection molding

Hamdy Hassan*, Nicolas Regnier, Cédric Le Bot, Guy Defaye

TREFLE Laboratory, Bordeaux1-UMR 8508, site ENSCPB, 16 av Pey Berland, 33607, Pessac Cedex, France

ARTICLE INFO

Article history:
Received 30 January 2009
Received in revised form
28 June 2009
Accepted 2 July 2009
Available online 28 July 2009

Keywords:
Cooling system
Injection molding
Polymer
Solidification
Heat transfer

ABSTRACT

The aim of the cooling system of a plastic injection mold is to provide thermal regulation in the injection molding process. When the hot plastic melt enters the mold cavity, it cools down and solidifies by dissipating heat through the cooling system. To study the effect of the cooling system design on the solidification and heat transfer of polymer by injection molding, a full three-dimensional time-dependent injection molding numerical analysis is carried out. The configuration studied consists of the mold with cuboids-shape cavity having two different thicknesses. The cooling of the polymer material is carried out by cooling water flowing through horizontal six cooling channels. A numerical model by finite volume is used for the solution of the physical model. A validation of the numerical model is presented. The effect of the cooling channels position and their cross-section shape on the cooling process is carried out. The results indicate that, for the same cross-sectional area and coolant flow rate of the cooling channels, the cooling channels having the form rectangular perform the minimum time required to completely solidify the plastic product. They also indicate that when the cooling channels approach to the product surface, the cooling efficiency increases.

1. Introduction

Plastic industry is one of the world's fastest growing industries, ranked as one of the few billion-dollar industries. Almost every product that is used in daily life involves the usage of plastic and most of these products can be produced by plastic injection molding method [1]. Injection molding represents the most important process for manufacturing plastic parts. It is suitable for mass-producing products, since raw material can be converted into a molding by single procedure [2]. Then, the plastic injection molding process is a cyclic process. It begins with feeding the resin and the appropriate additives from the hopper to the heating/injection system of the injection molding machine. The mold cavity is filled with hot polymer melt at injection temperature (filling stage). After the cavity is filled, additional polymer melt is packed into the cavity at a higher pressure to compensate the expected shrinkage when the polymer solidifies (post filling stage), since the post filling (holding) pressure is about 50–70% the injection pressure. This is followed by "cooling stage" where the mold is cooled until the part is sufficiently rigid to be ejected. The last step is the ejection stage where the mold is opened and the part is ejected. Then the mold is closed again to begin the next cycle [3]. Many aspects of production efficiency and part quality are significantly affected by the mold cooling process.

Cooling system is of great importance for plastic products industry by injection molding. It is crucial not only to reduce molding cycle time but also it extensively affects the productivity and the quality of the final product. The cooling system must be able to remove the heat at the required rate so that the plastic part can be ejected without distortion. An efficient cooling system aiming at reducing cycle time and reducing operation cost, must minimize such undesired defects like sink marks, differential shrinkage, thermal residual stress built-up, and product warpage and achieves uniform temperature distribution through the product. As a result, cooling system design seeks to obtain a uniform temperature distribution at minimum cooling cycle time [4]. In addition to the functional aspects, the design of a cooling system should also consider the manufacturability of the system to control the cost of mold construction. Extensive research and commercial codes have been conducted into the analysis of cooling systems and to carry out these goals. The early work reported by Barone and Caulk [5] was the optimization arrangement of the circular holes in a heat conductor to maintain a uniform temperature distribution over single-cavity mold surface. They used the boundary element method and a certain type of whole element to simulate two-dimensional steady-state heat conduction problems. Tang et al. [4] presented a methodology for optimal cooling system

* Corresponding author. Tel.: +33 0540006348; fax: +33 0540002731.
E-mail addresses: hamdyaboali@yahoo.com, hassan@enscpb.fr (H. Hassan).

1290-0729/$ – see front matter © 2009 Elsevier Masson SAS. All rights reserved.
doi:10.1016/j.ijthermalsci.2009.07.006

Nomenclatures

B	polymer material constant, Pa s
C	fractional volume function
C_P	specific heat, J kg^{-1} K^{-1}
f_s	solid fraction
g	acceleration gravity, m s^{-2}
K	permeability, m^2
L	latent heat of fusion, J kg^{-1}
m	mass, kg
N	normal direction
n	power index
p	pressure, Pa
Q	flow rate, m^3 s^{-1}
S_c	source term, W m^{-3}
s	side length, m
T	temperature, K
t	time, s
T_b	polymer material constant, K
$\boldsymbol{V}$	velocity, m s^{-1}

Greek symbols

τ^*	critical stress level, Pa
μ	dynamic viscosity, Pa s
η	shear rate viscosity, Pa s
ϕ	viscous dissipation term, W m^{-3}
β	polymer material constant, Pa^{-1}
ρ	density, kg m^{-3}
λ	thermal conductivity, W m^{-1} K^{-1}
$\dot{\gamma}$	equivalent shear rate, s^{-1}
η_0	zero shear viscosity, Pa s
Γ_1	entry region to the mold cavity
Γ_2	entry region to the cooling channels

Subscripts

a	air
B	sensitivity parameter
c	cooling channels
f	melting
fin	final
l	liquid
i	initial
p	polymer
∞	ambient condition
s	solid

for multi-cavity injection mold tooling. The methodology optimizes cooling system layout in terms of cooling channel size, locations and coolant flow rate and their effect on the temperature distribution of the mold. Methods to build better cooling systems by using new forms of fabrication technology have been reported by Lin [6]. He illustrated a neural network approach for the modeling and optimization of injection-mold cooling systems parameters (cooling channels diameters, and their offset) and their effect on the warpage of the product. Qiao [7] presented a fully transient mold cooling analysis using the boundary element method based on the time-dependent fundamental solution for a two-dimensional cyclic transient analysis. He gave the temperature evolution with time along different positions at the cavity wall. A systematic computer-aided approach is developed by Qiao [8] to achieve the optimal design of the cooling system. He tried to obtain the optimum position for the cooling channels to cool a rectangular cavity. Li and Li [9] used a configuration space method (C-space) to underline the layout of the cooling channels design inside the mold. During these previous studies, the cavity is closed and completely filled with hot polymer and the filling stage is neglected.

In this paper, three-dimensional study is presented. The effect of the cooling channels position and their form on the solidification and temperature distribution are studied during the cooling of polystyrene material by injection molding. The mold cavity has the form of cuboids with two different thicknesses. Three forms of the cooling channels are assumed (circular, rectangular and square). Different locations of the cooling channels are taken in consideration during the study. The polymer material is cooled by six cooling channels as shown in Fig. 1 (dimensions in mm). A finite

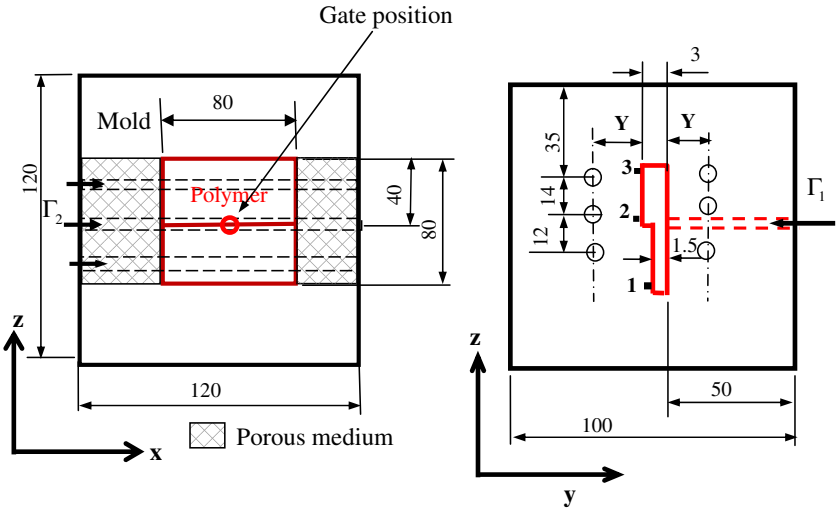

Fig. 1. Configuration of the mold, mold cavity and cooling channels.

volume model is used for the simulation of the physical model. A validation of the numerical model is presented.

2. Mathematical model

The mathematical equations governing the physical model must take into considerations: the injection of the polystyrene material into the mold cavity, the solidification of the polymer material during the cooling process, the flow of the cooling fluid inside the cooling channels.

During the filling, cooling, solidification and ejection of the product, the following assumptions are introduced for the mathematical model.

The polymer material and cooling fluid flowing inside the cooling channels are considered non-compressible fluids.

The physical and thermal properties (ρ, λ, C_P) of the polymer, mold, and cooling water are considered constant during the numerical simulation.

Generally, the mathematical equations governing the physical model are the classical generalized Newtonian model which are the mass, momentum and energy equations:

$$\nabla\cdot\boldsymbol{V} = 0 \tag{1}$$

$$\rho\left[\frac{\partial\boldsymbol{V}}{\partial t}+(\boldsymbol{V}\nabla)\cdot\boldsymbol{V}\right] = -\nabla P+\rho\boldsymbol{g}+\nabla\cdot\left[\eta\left(\nabla\boldsymbol{V}+\nabla^{\mathrm{T}}\boldsymbol{V}\right)\right] \tag{2}$$

$$\rho C_P\left[\frac{\partial T}{\partial t}+(\boldsymbol{V}\nabla)\cdot T\right] = \nabla\cdot(\lambda\nabla T)+\phi \tag{3}$$

where,

$$\phi = \eta\dot{\gamma}^2 \tag{4}$$

where ϕ represents the viscous dissipation term. In addition to the conservation laws, to take into consideration the polymer viscosity, the polymer viscosity is proposed as a function of shear rate, temperature, and pressure. A Cross type equation is used to describe the rheological behavior of the polymer material [10]:

$$\eta = \frac{\eta_0(T,p)}{1+\left[\eta_0(T,p)\frac{\dot{\gamma}}{\tau^*}\right]^{1-n}} \tag{5}$$

where τ^* is a critical stress level at which η is in transition between the Newtonian limits.

η_0 is expressed by an Arrhenius law with temperature sensitivity and exponential pressure dependence [9]:

$$\eta_0(T,p) = B\exp\left(\frac{T_b}{T}\right)\exp(\beta p) \tag{6}$$

The rheological model constants of the selected polystyrene material are listed in Table 1 [11].

The momentum equation is closely coupled with the viscosity constitutive relation. The following linear laws are adopted in this work to approximate the viscosity and density at the interface between the polymer melt and the air [12]:

$$\begin{cases}\rho = \rho_a+\left(\rho_p-\rho_a\right)C\\ \mu = \mu_a+\left(\mu_p-\mu_a\right)C\end{cases} \tag{7}$$

The fractional volume phase function C is defined as follows:

$$C = \begin{cases}1 & \text{for the point inside polymer}\\ 0 & \text{for the point inside air}\end{cases} \tag{8}$$

Then the interface is located within the cells where, $0<C<1$. The phase function is governed by a transport equation:

$$\frac{\partial C}{\partial t}+\boldsymbol{V}\cdot\nabla C = 0 \tag{9}$$

This equation determines the movement of interface position between the polymer and the air.

In order to take into account the solidification, a source term is added to the energy equation corresponding to heat absorption or heat release [13], which takes in consideration the absorption or the dissipation of the heat through phase change process. In this case the energy equation is solved with a fixed point algorithm for the solid fraction. For each iteration of that fixed point, we use discretization with time hybrid explicit/implicit technique already validated in previous studies by Le Bot [13] and it is based on the technique "New Source" of Voller [14]. This method proposes to maintain the nodes where phase change occurs to the melting temperature. This solution is repeated until the convergence of the temperature with the source term equals to the latent heat. The energy equation in this case is represented as follows:

$$\rho C_P\left[\frac{\partial T}{\partial t}+(\boldsymbol{V}\nabla)\cdot T\right] = \nabla\cdot(\lambda\nabla T)+\phi+S_c \tag{10}$$

where the source term S_c is represented by

$$S_c = \rho L\frac{\partial f_s}{\partial t} \tag{11}$$

where $f_s(T)=0.0$ at $T>T_f$ (fully liquid region), $0<f_s<1$ at $T=T_f$ (isothermal phase change region) and, $f_s(T)=1$ at $T<T_f$ (fully solid region).

This system of equations with the following boundary conditions is used to determine the different solution parameters (pressure, velocity, temperature, …) of the physical model.

At the inlet to the mold cavity:

During filling stage, constant inlet flow rate Q and isothermal conditions are used for the polymer.

$$Q = Q_p \text{ and } T = T_p \text{ on } \Gamma_1 \tag{12}$$

During cooling stage, zero inlet velocity and adiabatic condition for the temperature are assumed.

At the inlet to the cooling channels:

Constant inlet flow rate and isothermal conditions are imposed.

$$Q = Q_c \text{ and } T = T_\infty \text{ on } \Gamma_2 \tag{13}$$

At mold side walls adiabatic boundary conditions are assumed.

Table 1
The rheological model constants.

Material constant	PS
n	2.7×10^{-01}
τ^*, Pa	2.31×10^{04}
B, Pa s	3.04×10^{-9}
T_b, K	13,300
β, Pa^{-1}	3.5×10^{-8}

3. Numerical solution

The numerical solution of the mathematical model governing the behavior of the physical system is computed by finite volume method. The equations are solved by an implicit treatment for the

different terms of the equations system. The solution of the descretized equations are solved by an iterative algorithm of Augmented Lagrangian, which makes the pressure velocity coupling. In our numerical solution, we use the concept of a unique system of equations, which is solved, in the whole numerical domain (one fluid model). Penalization terms are added to the general system of equations to take into account different boundary conditions and solid mold zones [15]. Using this technique of unique system makes the numerical discretization simpler, easy to program.

3.1. Solid obstacles

To deal with solid mold within the numerical domain, it is possible to use multi-grid domains, but it is often very much simpler to implement the Brinkman theory [14]. The numerical domain is then considered as a unique porous medium. The permeability coefficient K defines the capability of a porous medium to let pass the fluids more or less freely through it. If this permeability coefficient is great ($K \to +\infty$), the Darcy term disappears and then we have the momentum equation (2) hence, the medium is equivalent to a fluid. If ($K \to 0$) the Darcy term will be dominant on the other terms and the velocity drops to zero, hence the medium is equivalent to a solid. A real porous medium is modeled with intermediate values of K. With this technique, it is possible to model moving rigid boundaries or complex geometries.

To take this coefficient K into account in our system of equations, an extra term, called Darcy term $(\mu/K)\boldsymbol{V}$ [15], is added to the momentum equation (2), and then the momentum equation becomes:

$$\rho\left[\frac{\partial \boldsymbol{V}}{\partial t}+(\boldsymbol{V}\nabla)\cdot\boldsymbol{V}\right]=-\nabla P+\rho\boldsymbol{g}+\nabla\cdot\left[\eta\left(\nabla\boldsymbol{V}+\nabla^{\mathrm{T}}\boldsymbol{V}\right)\right]-\frac{\mu}{K}\boldsymbol{V} \tag{14}$$

Practically, values of $K=10^{+20}\,\mathrm{m}^2$ and $K=10^{-20}\,\mathrm{m}^2$ are imposed to obtain these conditions, liquid and solid medium respectively and the values of K between $10^{+20}\,\mathrm{m}^2$ and $K=10^{-20}\,\mathrm{m}^2$ represents a real porous medium.

3.2. Boundary conditions

To deal with the boundary conditions within the numerical domain, the method consists in writing a generalized boundary condition as a surface flux [16]:

$$-\left(\frac{\partial \boldsymbol{V}}{\partial N}\right)_{\text{surface}}=B_V(\boldsymbol{V}-\boldsymbol{V}_\infty) \tag{15}$$

where B_V is a matrix. It has to be noted that it is a vectorial formulation and then involves the three Cartesian components of the velocity vector $\boldsymbol{V}$. The boundary condition is directly taken into account in equation (14), then we have the following equation

$$\rho\left[\frac{\partial \boldsymbol{V}}{\partial t}+(\boldsymbol{V}\nabla)\cdot\boldsymbol{V}\right]+B_V(\boldsymbol{V}-\boldsymbol{V}_\infty)=-\nabla P+\rho\boldsymbol{g}+\nabla\cdot\left[\eta\left(\nabla\boldsymbol{V}+\nabla^{\mathrm{T}}\boldsymbol{V}\right)\right]-\frac{\mu}{K}\boldsymbol{V} \tag{16}$$

Thanks to this penalization term, we can then impose a velocity in the numerical domain or on a lateral boundary. For $B_{\boldsymbol{V}}=0$, Neumann boundary conditions are modeled where $(\partial\boldsymbol{V}/\partial N)=0$. Some coefficients are chosen as $B_{\boldsymbol{V}}=+\infty$ to ensure Dirichlet boundary conditions imposed at the mesh grid points of the boundary. This formulation enables us to easily modify the boundary conditions while passing from the condition of Neumann to a condition of Dirichlet.

Table 2
Properties of the selected fluid.

Property	Unit	Liquid	Solid
Density, ρ	$\mathrm{Kg\,m^{-3}}$	998	998
Specific heat, C_p	$\mathrm{J\,kg^{-1}\,K^{-1}}$	4182	2037
Thermal conductivity, λ	$\mathrm{W\,m^{-1}\,K^{-1}}$	0.6	2.2
Latent heat, L	$\mathrm{J\,kg^{-1}}$	333,000	
Melting temperature	°C	0.0	

The same procedure is used to impose the boundary condition in case of the Energy equation. The quantity $B_T(T-T_\infty)$ is introduced in equation (10) and then the following equation for the energy is solved:

$$\rho C_P\left[\frac{\partial T}{\partial t}+(\boldsymbol{V}\nabla)\cdot T\right]+B_T(T-T_\infty)=\nabla\cdot(\lambda\nabla T)+\phi+S_c \tag{17}$$

where

$$B_T=0:\ \text{Neumann condition}\left(\frac{\partial T}{\partial N}=0\right) \tag{18}$$

$$B_T\to\infty:\ \text{Dirichiet condition}(T=T_\infty) \tag{19}$$

Further details on the numerical model are available in [17,18]. To validate this numerical model, analytical solutions known in cases of filling a square cavity, and a solidification of a liquid inside a closed square cavity is used.

3.3. Validation

The validation of the numerical solution in case of solidification is carried out for a case of square cavity model with side length S and total volume $S^2\times1$. It is assumed that the domain is filled with a material which can be solid or liquid. The properties of the selected fluid are shown in Table 2. The liquid phase represents a square cavity inside the whole domain with side length S_l and a total volume of $S_l^2\times1$, then the solid volume $(S^2\times1-S_l^2\times1)$. Then,

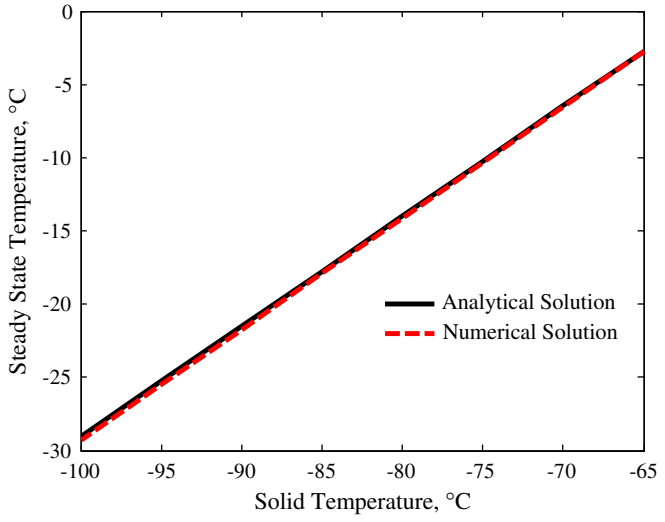

Fig. 2. Comparison between the analytical solution and numerical solution for the solidification case.

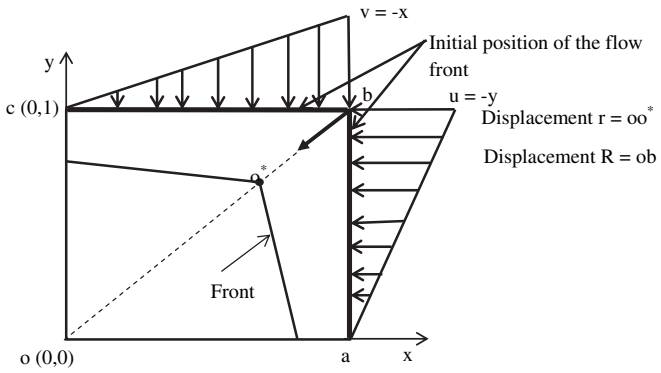

Fig. 3. Flow front through a square cavity within a given velocity field.

$$\text{Liquid mass is } m_l = \rho S_l^2 \times 1 \tag{20}$$

$$\text{Solid mass is } m_s = \rho S^2 \times 1 - m_l \tag{21}$$

The liquid domain is initially at temperature $T_i = 10\ ^\circ C$.
The final temperature at steady state is

$$T_{fin} = \frac{m_l(C_{Ps} - C_{Pl})T_f + m_l C_{Pl} T_l + m_s C_{Ps} T_s + m_l L}{(m_s + m_l)C_{ps}} \tag{23}$$

The numerical results compared with the analytical solution for the final steady state temperature is shown in Fig. 2. It represents the final steady state temperature for different initial solid domain temperatures T_s. The result indicates a good agreement between the two results for different initial solid temperatures.

Filling a square cavity:

The example consists in filling a unit square cavity where a velocity field is imposed at the boundary as shown in Fig. 3 [19]:

$$\boldsymbol{u} = -y \tag{24}$$

$$\boldsymbol{V} = -x$$

Since the velocity is steady, the particle pathlines and the streamlines are coincident, and governed by

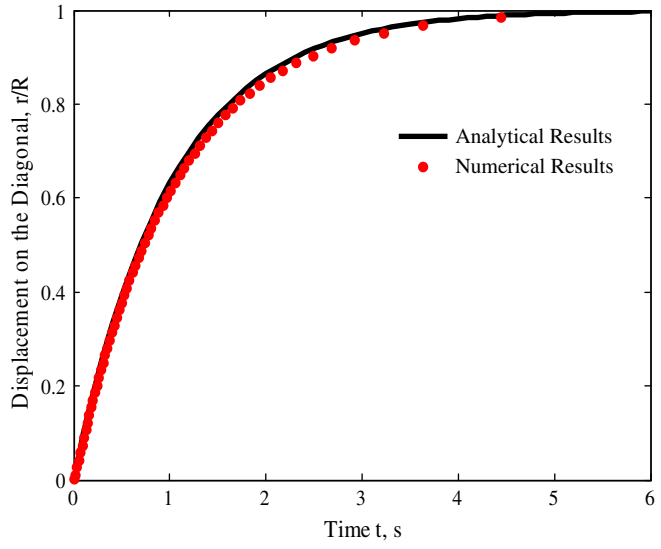

Fig. 4. Comparison of the numerical results with the analytical solution.

Table 3
Cooling operating parameters.

Cooling operating parameter		Cooling operating parameter	
Inlet temperature of the Coolant fluid	30 °C	Time of injection stage	4.2 s
Injected temperature of polymer	220 °C	Time of cooling stage	37.5 s
Fusion temperature of polymer	110 °C	Mold opening time	3 s
Latent heat	115 kJ kg^{-1} K^{-1}	Diameter of the circular cooling channels	8 mm
Temperature of ambient air	30 °C	Flow rate of cooling water	1e^{-4} m^3 s^{-1}

$$y^2 = x^2 + C_1 \tag{25}$$

where C_1 is a constant. The magnitude of the velocity vector $|\boldsymbol{U}|$ is equal to $(x^2 + y^2)^{1/2}$. The initial front is assumed as straight lines *ab* and *bc* as shown in Fig. 3. As the fluid fills the square cavity from the top and right sides, the velocity diminishes and vanishes at the origin *o*. Since the particle at the point *b* will flow along the square diagonal.

Then the analytical solution of the non-displacement (r/R) versus filling time (t) is [19]:

$$r/R = 1 - e^{-t} \tag{26}$$

where r is the particle displacement $|bo^*|$ and R is the length of the diagonal $|bo|$ as shown in Fig. 3.

Numerically, the initial condition is $V = 0$ and the other boundary conditions assumed for the cavity are Neumann.

In order to compare the numerical solution with the analytical solution, the flow front position at the diagonal is calculated at various times. A good agreement between the numerical solution and the analytical solution is obtained during the entire filling process as shown in Fig. 4.

4. Results and discussions

A full three-dimensional time-dependent injection molding analysis is carried out for a cuboids mold model with cuboids-cavity having two different thicknesses as shown in Fig. 1. The cooling of the product is carried out by using cooling water flowing through six cooling channels. All the cooling channels have the same size and they are 8-mm diameter in case of circular forms. The cooling operating parameters and the material properties are listed in Tables 3 and 4 respectively [7,11] and they are considered constant during all numerical simulation except illustrated within the text.

In our numerical model, each numerical simulation consists of three main stages (injection, cooling and ejection stages). During injection stage, hot polymer is injected to the mold cavity at constant temperature and constant flow rate. During cooling stage, the polymer injected is cooled until the end of cooling time. During

Table 4
Material properties.

Material	Density, kg m^{-3}	Specific heat, J kg^{-1} K^{-1}	Conductivity, W m^{-1} K^{-1}
Mold	7670	426	36.5
Polymer	938	2280	0.18
Cooling water	1000	4185	0.6
Air	1.17	1006	0.0263

the last stage (ejection stage), the cavity is assumed filled with air which is initially at ambient temperature.

The mold cavity must be completely filled with hot polymer, so it is assumed that the air escapes from the mold cavity through a thin layer of porous medium. This layer has the same properties of mold material with thickness of 1 mm as shown in Fig. 1. According to equation (16), the permeability factor K determines the capability of a porous medium to let the fluid pass more or less freely through it.

When a fluid moves in a porous medium, its macroscopic velocity does not check any more the conservation equation of momentum defined in equation (14). Darcy showed in experiments that the flow in a column filled with sand is proportional to the gradient of pressure imposed between two sections of the column and inversely proportional to the viscosity of the fluid, which runs out, and then the Darcy law is written as [20]

$$\boldsymbol{V} = -\frac{K}{\eta}\nabla P \tag{28}$$

Here $\boldsymbol{V}$ is the volume averaged flow velocity, ∇P is the pressure gradient across the porous medium, η is the viscosity of the fluid and K is the permeability of the porous medium.

By considering the air viscosity, the injection pressure, the time required to withdraw the air from the cavity (filling time), and the total volume of the mold cavity, it is found that the value of permeability K must not be less than 10^{-12} m^2. Fig. 5 shows the influence of the permeability factor K of the porous medium on the percentage of filled cavity volume and the inlet pressure to the cavity. It shows that when the permeability factor increases, the filled volume of the cavity with polymer material decreases. It also shows that when the value of K increases, the inlet pressure decreases. When the value of K increases, the polymer material would escape to the porous medium. Hence, because of the volume inters the cavity is constant, the filled volume of the cavity with polymer decreases. The value of K equals 1×10^{-10} m^2 is chosen which gives the maximum percentage of the cavity volume filled with polymer. It is also adequate for the air to escape from the mold cavity and it keeps the polymer inside the cavity during the filling process. Moreover, it provides at the inlet to the cavity a pressure equivalent to the pressure of the injection molding machine (25–75 MPa) [11] as shown in Fig. 5.

An efficient cooling system design provides uniform temperature distribution throughout the entire part during the cooling process. At the same time, it should reduce cooling time by accelerating the solidification process of the product to augment the productivity of the molding process. After demolding, the residual stresses (thermal and flow induced stress) will redistribute and cause the part shrinkage and warpage. Thermal induced residual stress is caused by non-uniform cooling of the molding part [21]. To study the effect of the cooling system, two parameters are considered: cooling channel positions and cooling channels form.

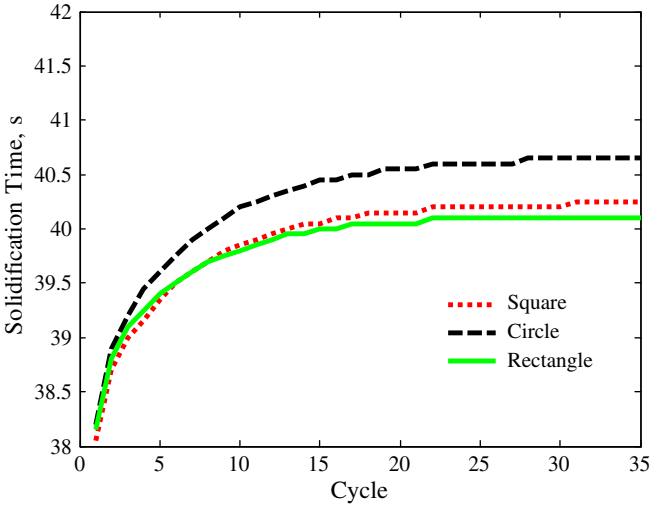

Fig. 6. The variation of the solidification time required to completely solidify the product with injection molding cycle at different cooling channels form.

4.1. Effect of cooling channels form

The form of the cooling channels with the same cross-section affects on the heat transfer between the cooling water and the mold because they have not the same perimeter and have not the same pressure drop and hence it affects on the cooling process of the polymer. To demonstrate the influence of the cooling channels form on the heat transfer of the product, we proposed three different cross-sectional forms of the cooling channels, circular, square and rectangular with long to width ratio of 0.5 All the cooling channels have the same cross-sectional area and the same flow rate of the

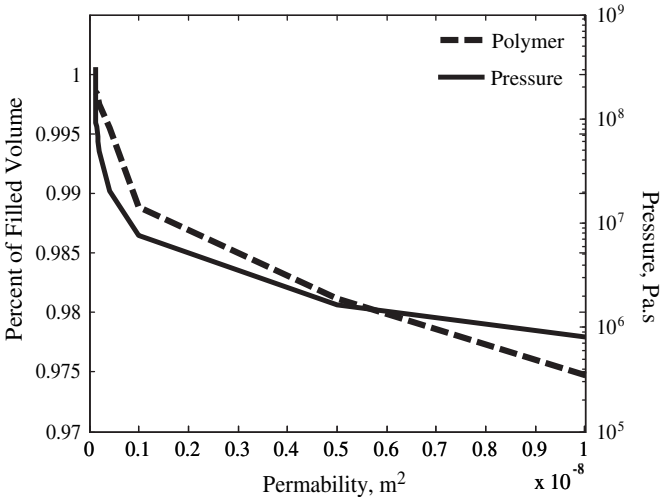

Fig. 5. Changing the percent volume filled – and inlet pressure to the cavity – with changing of permeability factor.

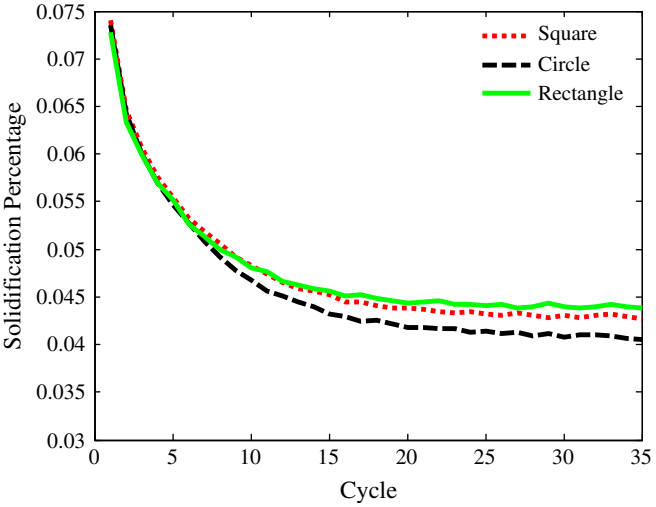

Fig. 7. The variation of the solidification percentage of the product at the end of filling stage with injection molding cycle at different cooling channels form.

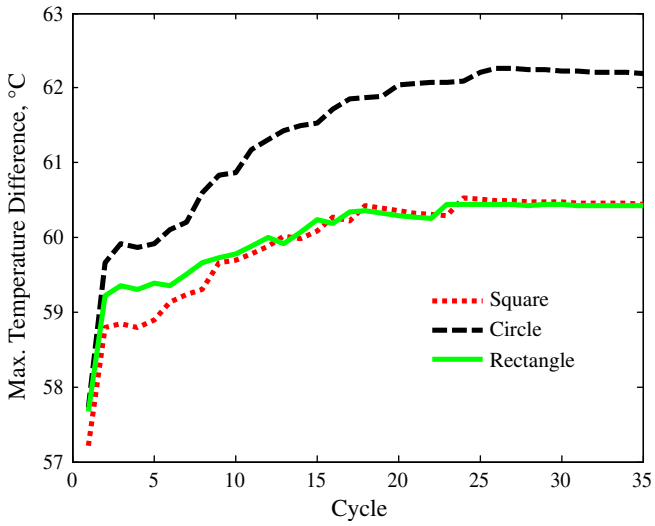

Fig. 8. The variation of the maximum temperature difference within the product at the end of cooling stage with injection molding cycle at different cooling channels form.

cooling water. The comparison is carried out for cooling channels positioned $Y = 8$ mm as shown in Fig. 1. All other process parameters are the same for the three forms. The simulation is performed for the first 35 cycles of injection molding.

Decreasing time spent on cooling the product before it is ejected, would drastically increase the production rate, and hence would reduce costs. It is therefore important to understand and thereby optimize the heat transfer processes within a typical molding process efficiently. The variation of the time required to completely solidify the product at each injection molding cycle for the different cooling channels form is shown in Fig. 6. Fig. 6 indicates that the mold having the rectangular cooling channels leads to the smallest total solidification time. It also shows that the time required to solidify the product decreases by about 1.5% for the rectangular form of cooling channels compared with other forms. To completely fill the mold cavity and minimize injection pressure; the solidification of the product during the injection stage must be avoided as possible. Fig. 7 shows the variation of the solidification percentage at the end of injection stage at each injection molding cycle. It shows that the mold having circular cooling channels has the minimum solidification percentage of the product at the end of filling stage and the mold with rectangular cooling channels has the maximum solidification percentage for each injection molding cycle. It also shows that the solidification of the product during the filling stage decreases with the progress of injection molding cycle due to the mold heating. These results indicate that if the cooling channels could be made to conform to the shape of the part as much as possible, then the cooling process is improved.

The final form and properties of the product depend on the average temperature of the product when it exits from the mold and the temperature distribution through the product. The maximum temperature difference (MTD) through the product is used to express the temperature of the product when it exits from

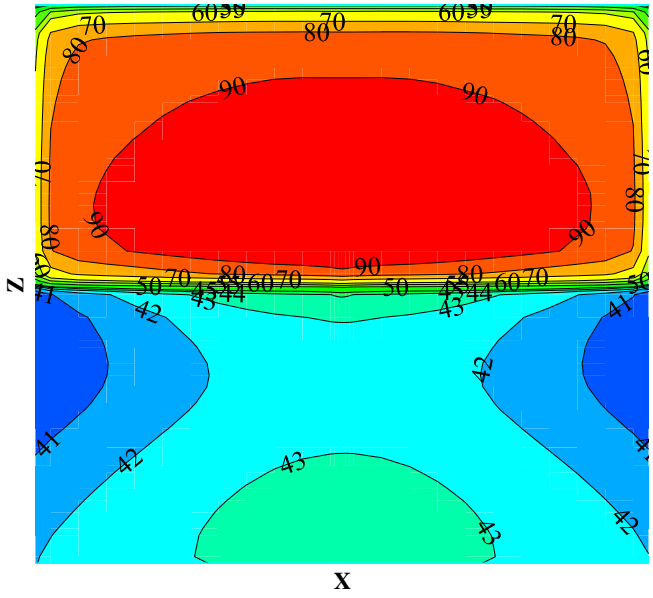

Fig. 10. Temperature distribution at plane xz and $y = 0.0485$ m through the product at the end of cooling stage of the 34th cycle for circular cooling channel.

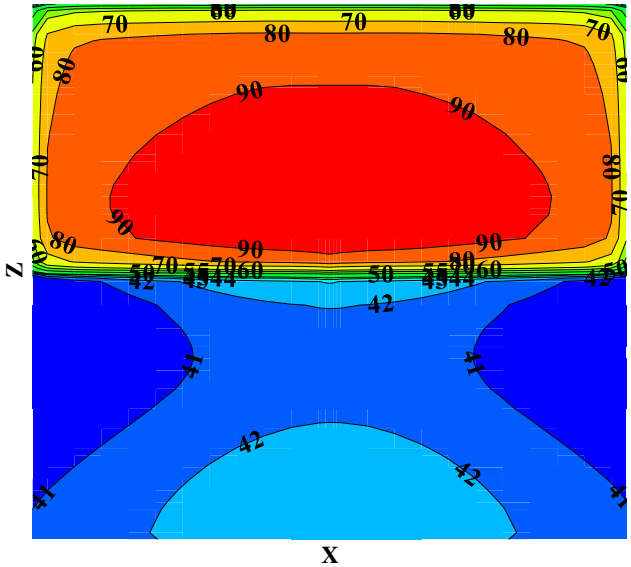

Fig. 9. Temperature distribution at plane xz and $y = 0.0485$ m through the product at the end of cooling stage of the 34th cycle for square cooling channel.

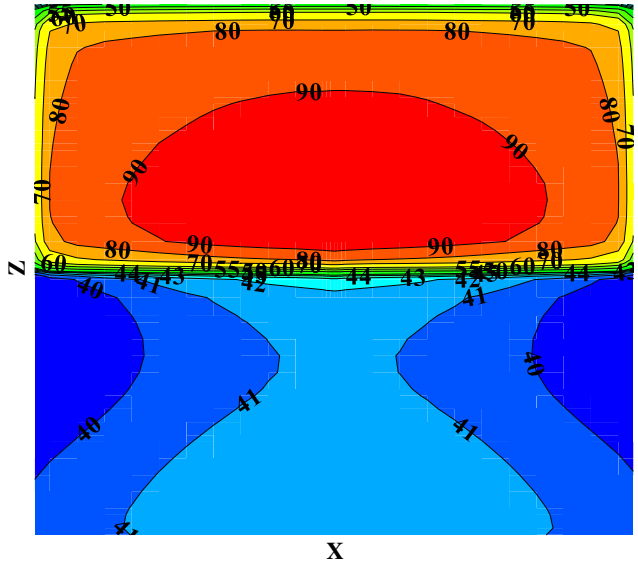

Fig. 11. Temperature distribution at plane xz and $y = 0.0485$ m through the product at the end of cooling stage of the 34th cycle for rectangular cooling channel.

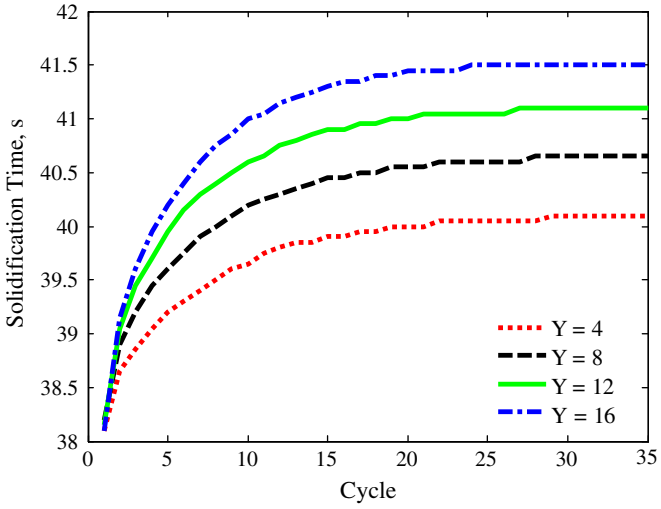

Fig. 12. The variation of the solidification time required to completely solidify the product with injection molding cycle at various cooling channels position.

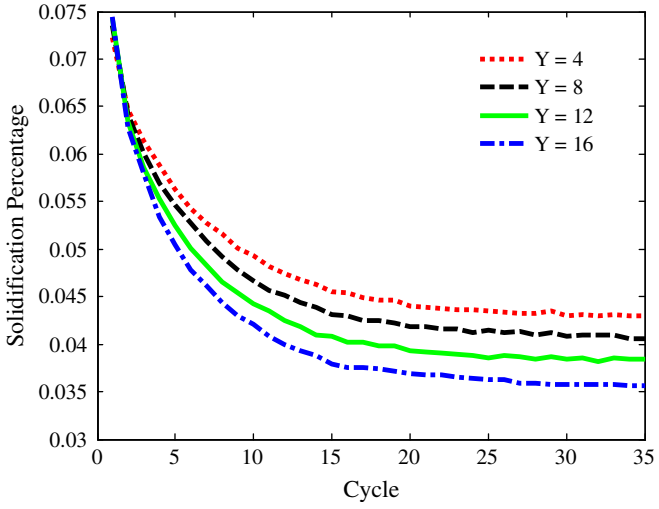

Fig. 14. The variation of the solidification percentage of the product at the end of filling stage with injection molding cycle at various cooling channels position.

the mold. This means that when the product exits from the mold with a minimum MTD, the final shape of the product takes the required form from it. Fig. 8 shows the variation of the MTD inside the product at the end of cooling stage with injection molding cycle. It shows that in case of circular cooling channels, the ejected product has the greater value of MTD. It also shows that in case of rectangular and square forms, the cooling channels have almost the same value of MTD. The temperature distribution through the *xz* plane and $y = 0.0485$ m (Fig. 1) of the product at the end of cooling stage of the 34th cycle for the injection molding in case of square, circular and rectangular cooling channels are shown in Figs. 9–11 respectively. The results show that the temperature distribution throughout the polymer divided into two regions (hot region for thick part and cold for thin part) during the cooling process. These two regions of the temperature distribution after demolding lead to different severe warpage and thermal residual stress in the final product. These thermal residual stress and severe warpage affect negatively on the final product quality. The different of the temperature of the thick part and the thin part demands increasing the cooling of thick part to reach a uniform temperature distribution throughout the product. In case of rectangular cooling channels, there is greater difference in the temperature between the thin and the thick part than in case of the other forms. From the analysis of the temperature distribution (Figs. 9–11), it is found that the thin part is greatly affected by cooling channel form than the thick part.

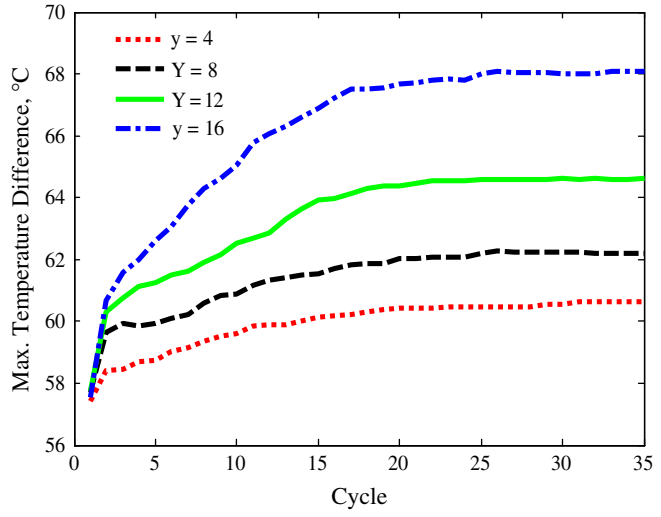

Fig. 13. The variation of the maximum temperature difference within the product at the end of cooling stage with injection molding cycle at various cooling channels position.

4.2. *Effect of cooling channels position*

The position of the cooling channels determines the amount of heat of the molten polymer taken away by forced convection to the coolant moving through the cooling channels. All the cooling channels have the same circular cross-section form. To investigate the effect of the cooling channels position, we divided the proposed positions into four groups ($Y = 4$, 8, 12 and 16 mm) as shown in Fig. 1. The time required to completely solidify the product for different cycles at different cooling channels position is shown in Fig. 12. The figure shows that when the cooling channels are close to the product, the time required for solidifying the products

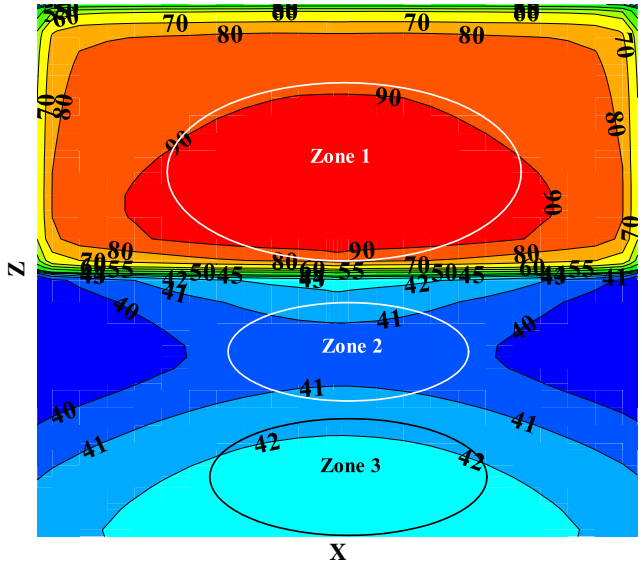

Fig. 15. Temperature distribution at plane *xz* and $y = 0.0485$ m through the product at the end of cooling stage of the 34th cycle for cooling channels position $Y = 4$.

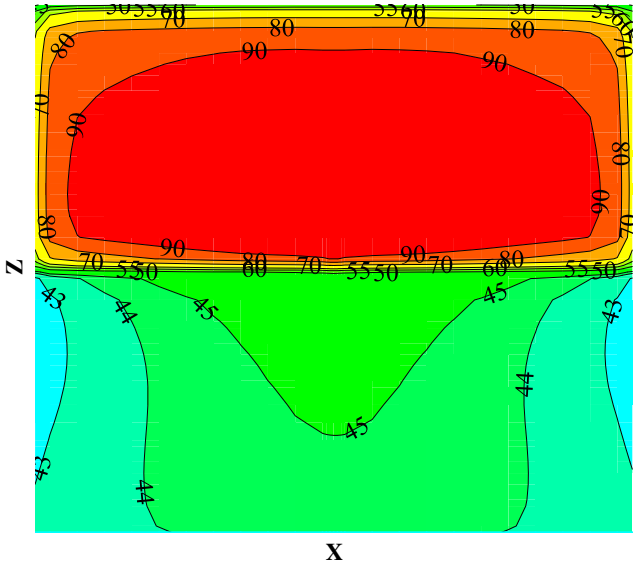

Fig. 16. Temperature distribution at plane xz and $y = 0.0485$ m through the product at the end of cooling stage of the 34th cycle for cooling channels position $Y = 16$.

decreases. They also show that by decreasing the distance between the cooling channels and the product by 400%, the cooling time required for solidification the product decreases by about 3.5%. The effect of the cooling channels position on the maximum temperature difference inside the product at the end of cooling stage and the solidification percentage of the product at the end of filling stage are shown in Figs. 13 and 14 respectively. Fig. 13 shows that when the cooling channels are close to the product, the maximum temperature difference within the product decreases. Another effect of the cooling channel position is that when the cooling channels approach to the surface of the product the solidification of the product increases during filling the cavity of the injection molding as shown in Fig. 14. The solidification of the product during the filling prevents the cavity to be filled completely with polymer material.

During cooling, location near the cooling channel experiences more cooling than a location far away from the cooling channel. This different temperature causes the material to experience differential shrinkage that causes thermal stresses. Significant thermal stress can cause warpage problem [22]. Therefore, it is important to simulate the temperature distribution due to the position of the cooling channels. The temperature distribution through the xz plane and $y = 0.0485$ m at the end of cooling stage of the 34th injection molding cycle for cooling channels position $Y = 4$ mm and $Y = 16$ mm are shown in Figs. 15 and 16 respectively. Fig. 15 indicates that when the cooling channels approaches to the product, the temperature distribution through the product divides into three zones. Zone 2 has the minimum temperature distribution because it has a small thickness and its position is close to the cooling channel. Compressive stress is developed at the location of fast cooling (zone 2) due to more shrinkage and caused warpage due to uneven shrinkage that happens. When the cooling channels departure from the product, the zones disappear and the temperature of the thin part approaches to that of the thick part (homogeneity increases) as shown in Fig. 16.

5. Conclusion

Three-dimensional study is carried out on the heat transfer of injected material having cuboids shape with two different thickness by injection molding. The cooling of the injected material is performed by cooling water flowing through six cooling channels inside the mold. The effect of the cooling channels position and their form on the heat transfer process through the product and the mold is studied. The results show that in case of rectangular cooling channel, the cooling process of the product is improved. They also indicate that when the cooling channels approaches to the product, the time required to completely solidify the product decreases by about 3%. The simulation shows that the cooling system layout which performs minimum cooling time not necessary achieves optimum temperature distribution throughout the product, and the system layout must be optimized to achieve the both goals. With this thermal analysis of the cooling system effect on the heat transfer process and a supplementary analysis on his effect on the warpage and residual stresses of the final product, would help in determining an optimum cooling system.

References

[1] S.H. Tang, Y.M. Kong, S.M. Sapuan, R. Samin, S. Sulaiman, Design and thermal analysis of plastic injection mold, J. Mater. Process. Technol. 171 (2006) 259–267.
[2] Seong-Yeol Han, Jin-Kuan Kwag, Cheol-Ju Kim, Tae-Won Park, Yeong-Deug jeong, Yeong-Deug Jeong, A new process of gas-assisted injection molding for faster cooling, J. Mater. Process. Technol. 155 (2004) 1201–1206.
[3] A.T. Bozdana, O. Eyercıoglu, Development of an expert system for the determination of injection moulding parameters of thermoplastic materials: EXPIMM, J. Mater. Process. Technol. 128 (2002) 113–122.
[4] Li Q. Tang, Constantin Chassapis, Souran Manoochehri, Optimal cooling system design for multi-cavity injection molding, Finite Elem. Anal. Des. 26 (1997) 229–251.
[5] M.R. Barone, D.A. Caulk, Special boundary integral equations for approximate solution of Laplace's equation in two-dimensional regions with circular holes, Q. J. Mech. Appl. Math. 34 (1981) 265–286.
[6] J.C. Lin, Optimum cooling system design of a free-form injection mold using an abductive network, J. Mater. Process. Technol. 120 (2002) 226–236.
[7] H. Qiao, Transient mold cooling analysis using the BEM with the time-dependent fundamental solution, Int. Comm. Heat Mass Tran. 32 (2005) 315–322.
[8] H. Qiao, A systematic computer-aided approach to cooling system optimal design in plastic injection molding, Int. J. Mech. Sci. 48 (2006) 430–439.
[9] C.G. Li, C.L. Li, Plastic injection mold cooling system design by the configuration space method, Comput. Aided Des. 40 (2008) 334–349.
[10] H.H. Chiang, C.A. Hieber, K.K. Wang, A unified simulation of the filling and post filling stages in injection molding. Part I: formulation, Polym. Eng. Sci. 31 (1991) 116–124.
[11] R. Luısa Alexandra, Viscoelastic compressible flow and applications in 3D injection moulding simulation, Ph.D. thesis, L'école national superiere des mines des Paris, 2004.
[12] S. Vincent, Modélisation d'écoulements incompressibles des fluides non miscibles, Ph.D. thesis, Bordeaux 1 University, Bordeaux, 1999.
[13] Le Bot, Impact et Solidification de Gouttes Métalliques sur un Substrat Solide, Ph.D. thesis, Bordeaux 1 University, Bordeaux, 2003.
[14] V.R. Voller, Fast implicit difference method for the analysis of phase change problems, Numer. Heat Trans. 17 (Part B) (1990) 155–169.
[15] E. Arquis, J.P. Caltagirone, Sur Les Conditions Hydrodynamiques au Voisinage d'une Interface Milieu Fluide-Milieu Poreux: Application à la Convection Naturelle, C.R. Acad. Sci. Sér. IIb 299 (1984) 1–4.
[16] S. Vincent, J.P. Caltgirone, A one-cell local multi-grid method for solving unsteady incompressible multiphase flows, J. Comput. Phys. 163 (2000) 172–215.
[17] Ph. Angot, Contribution à l'étude des Transferts Thermiques Dans les Systèmes Complexes, Application aux Composants Électroniques, Ph.D. thesis, Bordeaux 1 University, Bordeaux, 1989.
[18] K. Khadra, Méthodes Adaptatives de Raffinement Local Multi Grille, Applications aux Équations de Navier–Stokes et de l'énergie, Ph.D. thesis, Bordeaux 1 University, Bordeaux, 1994.
[19] D.M. Gao, A three dimensional hybrid finite element-volume tracking model for mould filling in casting process, Int. J. Numer. Meth. Fluids 29 (1999) 877–895.
[20] Pavel Simacek, Suresh G. Advani, Gate elements at injection locations in numerical simulations of flow through porous media: application to mold filling, Int. J. Numer. Meth. Eng. 61 (2004) 1501–1519.
[21] Tong-Hong Wang, Wen-Bin Young, Study on residual stresses of thin-walled injection molding, Eur. Polymer J. 41 (2005) 2511–2517.
[22] X. Chen, Y.C. Lam, D.Q. Li, Analysis of thermal residual stress in plastic injection molding, J. Mater. Process. Technol. 101 (2000) 275–280.